Pediatric Radiology (2024) 54:758–763
https://doi.org/10.1007/s00247-024-05862-3

ORIGINAL ARTICLE

Impact of beam collimation of z-overscanning on dose to the lens and thyroid gland in paediatric thoracic computed tomography imaging

Takanori Masuda[1] · Masao Kiguchi[2] · Chikako Fujioka[2] · Takayuki Oku[3] · Toru Ishibashi[3] · Yasushi Katsunuma[4] · Takayasu Yoshitake[5] · Shuji Abe[6] · Kazuo Awai[7]

Received: 31 August 2023 / Revised: 17 January 2024 / Accepted: 19 January 2024 / Published online: 3 February 2024

Abstract

Background Adaptive collimation reduces the dose deposited outside the imaged volume along the z-axis. An increase in the dose deposited outside the imaged volume (to the lens and thyroid) in the z-axis direction is a concern in paediatric computed tomography (CT).

Objective To compare the dose deposited outside the imaged volume (to the lens and thyroid) between 40-mm and 80-mm collimation during thoracic paediatric helical CT.

Materials and methods We used anthropomorphic phantoms of newborns and 5-year-olds with 40-mm and 80-mm collimation during helical CT. We compared the measured dose deposited outside the imaged volume using optically stimulated luminescence dosimeters (OSLD) at the surfaces of the lens and thyroid and the image noise between the 40-mm and 80-mm collimations.

Results There were significant differences in the dose deposited outside the imaged volume (to the lens and thyroid) between the 40-mm and 80-mm collimations for both phantoms ($P < 0.01$).

Conclusion Compared with that observed for 80-mm collimation in helical CT scans of the paediatric thorax, the dose deposited outside the imaged volume (to the lens and thyroid) was significantly lower in newborns and 5-year-olds with 40-mm collimation.

Keywords Beam collimation · Computed tomography · Lens · Paediatrics · Thyroid

Introduction

Prior to the development of multidetector computed tomography (CT), paediatric chest imaging was difficult to perform on children with congenital heart disease. With the recent developments in CT equipment, the technical performance of CT has improved dramatically over the past two decades [1–3]. Significant improvements in temporal resolution, including shorter rotation times [4, 5], a high helical pitch [6, 7], and wide detectors [8, 9], have proven effective in reducing artefacts associated with high heart rates and motion. These advancements have substantially improved the diagnostic capabilities of congenital heart diseases in children [10]. However, one cause of unnecessary exposure, often cited as significantly contributing to the total dose during helical thoracic CT examination, is the z-over scanning effect [11–15]. Z-over scanning is associated with helical CT and is related to the fact that the z-interpolation

✉ Takanori Masuda
takanorimasuda@yahoo.co.jp

1 Department of Radiological Technology, Faculty of Health Science and Technology, Kawasaki University of Medical Welfare, Matsushima, Kurashiki, Okayama 288701-0193, Japan

2 Department of Radiology, Hiroshima University, Hiroshima, Japan

3 Department of Radiological Technologist, Tsuchiya General Hospital, Hiroshima, Japan

4 Department of Radiological Technology, Tokai University Oiso Hospital, Kanagawa, Japan

5 TOWCAR WORKS Co., Ltd, Oita, Japan

6 Department of Radiological Technology, Osaka College of High Technology, Osaka, Japan

7 Department of Diagnostic Radiology, Hiroshima University, Hiroshima, Japan

necessary for image reconstruction requires data to be acquired above and below each image position [16, 17]. For a given scan length covered in the helical mode, at least half of the rotation (180° in parallel ray geometry) is necessary at the beginning and end of the scan to ensure that complete datasets are obtained for the reconstruction of the first and last sections [18]. Therefore, adaptive collimation is used to reduce the dose deposited outside the imaged volume in the z-axis direction. The highest dose deposited outside the imaged volume on CT arises from internal rather than external scatter. Therefore, an increase in the dose deposited outside the imaged volumed to the lens along the z-axis is a concern in paediatric thoracic CT.

The International Commission on Radiological Protection (ICRP) Publication 118 reported that the lens of the eye is one of the most radiosensitive tissues [19, 20]. Several recent studies have suggested a low threshold for radiation-induced cataracts [21, 22]. It has also been suggested that no such threshold may exist [23]. The precise mechanism of radiation cataractogenesis is unknown; however, genomic damage resulting in altered cell division, transcription, and abnormal lens fibre cell differentiation is considered salient. Human epidemiological studies and recent experiments on radiation cataracts in animals suggest that the triggering biological processes for the initial development of radiation-induced cataracts may occur following exposure to very low doses of radiation. The effect of the dose deposited outside the imaged volume on cataracts in children remains unknown. Publication 103 of the ICRP in 2007 reviewed recent data on radiation damage to the lens and may change the dose limits in the future [24]. There have been few reports of radiation damage to the lens, especially in children. Special attention must be paid to the lens radiation dose in paediatric CT scans because the life expectancy of children is higher than that of adults. Thyroid dose reduction is also important, particularly in the paediatric population [25]. From the perspective of radiological protection, these effects can be divided into stochastic and deterministic (threshold). The primary concern for the lens is deterministic effects (e.g. cataracts), whereas that for the thyroid is stochastic effects (e.g. cancer). An adaptive collimation method was developed to reduce the dose deposited outside the imaged volume in the z-axis direction during helical scanning. It has been reported [26] that a 50% reduction in the dose deposited outside the imaged volume can be achieved using adaptive collimation. However, the difference in the dose deposited outside the imaged volume to the lens has not been investigated between 40-mm and 80-mm collimation during thoracic paediatric helical CT.

This study aimed to compare the dose deposited to the lens and thyroid outside the imaged volume between 40-mm and 80-mm collimation during thoracic paediatric helical CT.

Methods

Computed tomography scanning parameters

Two paediatric anthropomorphic phantoms (ATOM Phantom, CIRS, Norfolk, VA) representing newborns and 5-year-olds were used in this study (Fig. 1). The weight and height of the newborn were assumed to be 3.5 kg and 51.0 cm, respectively, and those of the 5-year-old were assumed to be 19.0 kg and 110.0 cm, respectively.

Paediatric anthropomorphic phantoms were scanned using a clinical helical scanner (Revolution CT, GE Healthcare, Waukesha, WI) from above the apex of the lung to

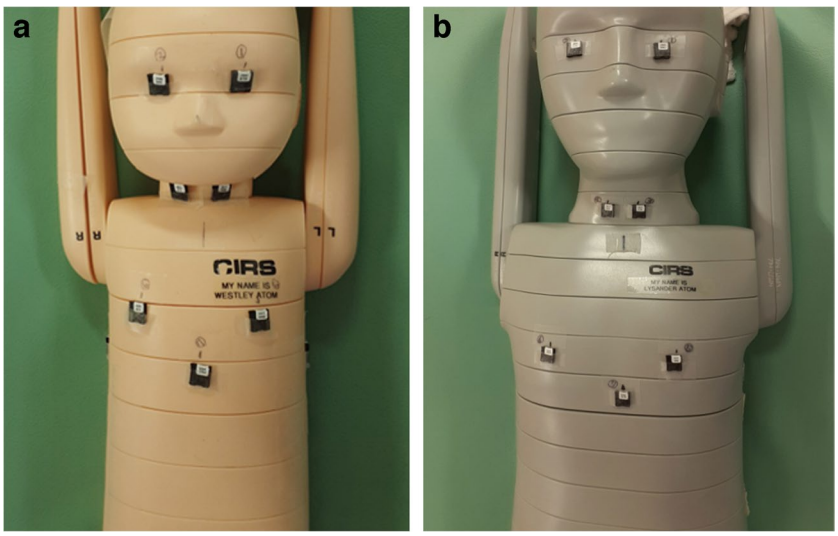

Fig. 1 Newborn (**a**) and 5-year-old (**b**) anthropometric phantoms (ATOM Phantom, CIRS, Norfolk) show the positioning of the optically stimulated luminescence dosimeter attachments

below the diaphragm. The scan range was 160 mm (Fig. 2). The scanning area was configured to avoid direct imaging of the thyroid gland. The scanning parameters were as follows: helical mode, beam collimation of 40 mm or 80 mm, section thickness of 5 mm, gantry rotation time of 0.5 s, and 64 × 0.625 mm or 128 × 0.625 mm detector collimation; settings for the small scan field of view of 100-mm matrix size was 512 × 512 for full mode and standard reconstruction kernel. The applied tube voltage was 80 kVp with automatic tube current modulation (noise index 10), and the helical pitches were 0.984 and 0.992 for the 40-mm and 80-mm beam collimations, respectively. The CT images were acquired using filtered back-projection algorithms with a standard kernel/filter.

Dosimeters and dose measurement

The optically stimulated luminescence dosimeters (OSLDs) used are commercial nanodot dosimeters (Landauer, Glenwood, IL) with a 5-mm diameter and 0.2-mm thick Al2O3:C disc, and were locally assessed. These discs were encased in a 10 mm × 10 mm × 2 mm light-sealed plastic case to prevent attenuation of the optical signal by light. According to the technical specifications of the OSLDs, the dose operating range is 5 mRad to 1500 rad (50 μGy to 1500 cGy). The lower limit of detection is 5 mRad (50 μGy). The useful energy range is from 5 keV to 20 MeV. Energy dependence is accurate within ± 10% over the diagnostic energy range of 70–140 kVp. The accuracy (total uncertainty, single measurement) is ± 10%. An InLight MicroStar reader (Landauer, Inc.) was used to read the optical signals from the OSLDs. The reader system included an optical annealing unit.

Anthropomorphic phantoms were placed on the CT scanner gantry, and an OSLD was placed on the right and left lenses, front sides of the right and left thyroid, and front sides of the right and left mammary glands, as well as front, back, right, and left sides of the mammary glands (Fig. 1). The mammary glands were in the field of view, and therefore data related to the mammary glands are not included in this study, although we did measure the dose to the mammary glands because they are highly susceptible to radiation-induced cancer. To ensure consistency in the placement of the discs for different scans, the dosimeters were affixed by a single researcher (T.M.) with 27 years of experience in CT. The OSLDs were affixed to paediatric anthropomorphic phantoms which were then consecutively scanned five times. Three sets of five consecutive scans (15 scans in total) were performed to mitigate errors from individual scans. The total dose acquired from five consecutive scans was divided by five to determine the average dose per scan. After each of the five consecutive scans, the OSLDs were replaced. During the helical scan, the measured doses deposited outside the imaged volumes were compared for each phantom between the 40-mm and 80-mm detector widths.

We comprehensively analysed radiation doses involving a 10-cm ionisation chamber and CT dose index volume (CTDIvol) obtained from the dose displayed on the console of our CT equipment. Furthermore, we extended our scrutiny to encompass a comparison of radiation doses using the 10-cm ionisation chamber and OSLDs when exposed to X-rays from general radiographic equipment. This evaluation was motivated by the need to assess the reliability of OSLDs.

Measurement of image noise and statistical analysis

For all paediatric phantoms, we measured the image noise (standard deviation [SD] of the CT number) at the level of the mammary gland in the centre of the scan range within a circumscribed 10.0-mm diameter region of interest (Fig. 3). For each scan, we measured the image noise five times at five peripheral and central points. The mean value of the SD of the CT number was calculated, and the

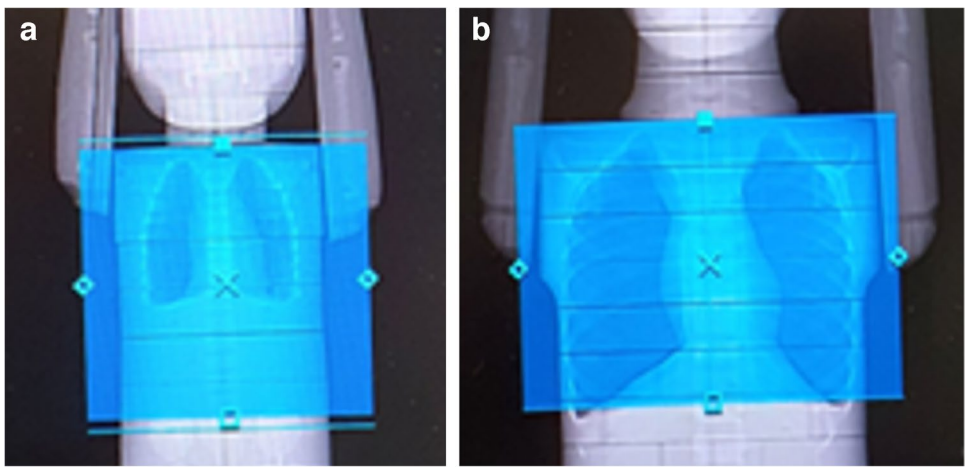

Fig. 2 Scan ranges for the anthropometric phantoms of a newborn (**a**) and a 5-year-old (**b**) are shown on scout views

image noise was compared for collimations of 40 mm and 80 mm.

The Mann–Whitney *U* test was used to analyse the dose deposited outside the imaged volume values for both phantoms. Statistical significance was set at $P < 0.05$. Statistical analyses were performed using the free statistical software "R" (R, version 3.2.2; R Project for Statistical Computing; http://www.r-project.org/).

Results

The doses deposited outside the imaged volume measured for both phantoms and collimations are summarised in Table 1 and Supplementary Material 1. Significant differences were observed in the dose deposited to the lens and thyroid between the 40- and 80-mm collimations for both phantoms ($P < 0.01$). However, there were no significant differences in CTDIvol between the 40- and 80-mm collimations for both phantoms (Table 1).

There were no significant differences in image noise between 40-mm and 80-mm collimation on helical scans in newborns and 5-year-olds ($P = 0.11$ and 0.14, respectively) (Table 2).

Discussion

This phantom study has shown that in newborns and 5-year-olds , the dose deposited outside the imaged volume (to the lens and thyroid gland) during thoracic helical CT, is significantly higher with 80-mm compared to 40-mm collimation.

Notably, our results show that compared with the 80-mm collimation, 40-mm collimation reduces paediatric lens doses. Deak et al. [27] reported that a substantial dose reduction was achieved for cardiac and thoracic CT using adaptive section collimation when measurements were performed in free air and phantoms. However, this effect increases with the number of detector rows, such as the function of the 40-mm collimation with less Z-plane over scanning unlike that of the 80-mm collimation.

During helical scanning, the dose deposited outside the imaged volume (to the lens) decreases with age. This

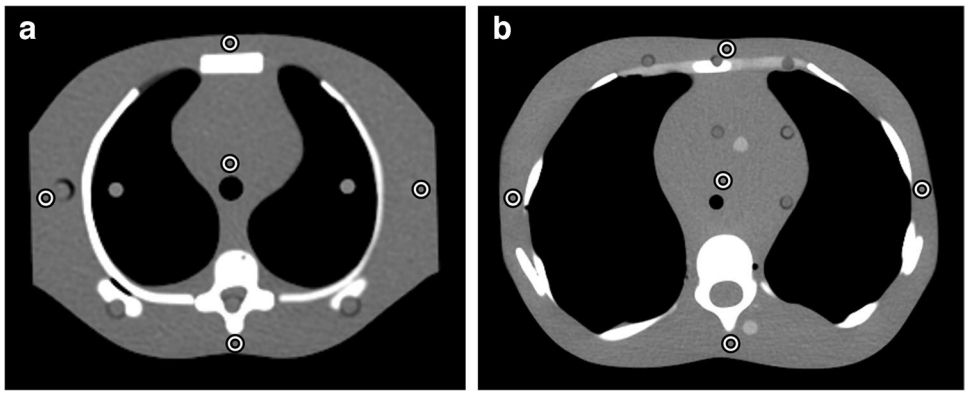

Fig. 3 Regions of interest measured for image noise in anthropomorphic newborn (**a**) and 5-year-old (**b**) phantoms

Table 1 Scatter radiation doses (median and interquartile range) for newborn and 5-year-old anthropomorphic phantoms measured using 40-mm and 80-mm collimation during helical computed tomography scans of the thoracic region

Phantom	Collimation (40 mm)	Collimation (80 mm)	*P*-value
Newborn			
Left lens (mGy)	0.11 (0.11–0.12)	0.33 (0.28–0.34)	< 0.01
Right lens (mGy)	0.08 (0.05–0.14)	0.36 (0.34–0.36)	< 0.01
Left thyroid (mGy)	1.39 (0.26–1.41)	2.00 (1.64–2.38)	< 0.01
Right thyroid (mGy)	1.19 (0.71–1.67)	1.71 (1.04–1.87)	< 0.01
CTDIvol (mGy)	1.83 (1.32–2.27)	1.73 (0.81–2.03)	0.46
5-year-old			
Left lens (mGy)	0.14 (0.13–0.16)	0.18 (0.17–0.18)	< 0.01
Right lens (mGy)	0.15 (0.14–0.15)	0.18 (0.17–0.20)	< 0.01
Left thyroid (mGy)	3.16 (3.01–3.39)	4.29 (4.01–4.35)	< 0.01
Right thyroid (mGy)	3.59 (3.45–4.04)	4.36 (3.93–4.42)	< 0.01
CTDIvol (mGy)	4.26 (4.04–4.32)	4.42 (4.12–4.83)	0.32

CTDIvol computed tomography dose index volume

Table 2 Image noise (standard deviation of computed tomography (CT) Hounsfield units averaged over selected region of interest) for 5-mm slice thickness at the level of the mammary glands, from thoracic helical (CT) scans of newborn and 5-year-old anthropomorphic phantoms using 40- and 80-mm collimation

Phantom	40 mm collimation	80 mm collimation	*P*-value
Newborn	8.5 (8.3–8.6)	8.3 (8.2–8.5)	0.11
5-year-old	9.1 (8.9–9.3)	8.9 (8.7–9.2)	0.14

Data are presented as the medium and range for the interquartile range of the measured dose values

phenomenon is attributed to the fact that the larger the body size, the wider the distance between the scanning position and the lens. Our results showed no difference in image noise from the 80-mm collimation with helical scanning compared to that with the 40-mm collimation. With regard to lens doses and image quality, we believe that 80-mm collimation for helical scanning is more effective in older patients, while 40-mm collimation for helical scanning is more effective in younger patients.

Overscanning and overranging are well researched [28]. Manufacturers have different approaches for reducing radiation exposure, such as the helical reconstruction algorithm, additional filters, and sequential exposure to avoid lens irradiation [28]. The direct visualisation on the scout view of the possible surface-exposed region must also be stressed in daily practice. It is important to understand and use the various types of overscanning and ranging techniques.

In the assessment of complex cardiac malformations, motion artefacts affect image quality. It has been reported [29] that the accuracy of CT with a 40-detector-row CT scanner in diagnosing separate cardiovascular anomalies is 98%. High-speed scans with an 80-detector-row CT scanner are necessary for coronary artery- and sedation-free cases; however, dose reduction may be a better consideration in general congenital heart disease cases.

The scan range in children is shorter than that in adults, which leads to a reduced scan time. Consequently, even with shorter collimation in contrast enhancement examinations, the impact on contrast enhancement is expected to be minimal. Theoretically, a shorter collimation can be applied to CT with contrast agent injections in children.

According to our results, 40-mm beam collimation was able to reduce the absorbed thyroid dose. The absorbed dose with the 80-mm beam collimation was significantly higher than that with the 40-mm beam collimation. The 40-mm beam collimation reduced the out-of-field absorbed doses compared with the in-field absorbed dose. By using 40-mm beam collimation, it is possible to reduce the absorbed doses of the thyroid compared to the absorbed thyroid doses observed for 80-mm beam collimation during paediatric thoracic helical CT.

Our study has some limitations. We used anthropomorphic phantoms of a newborn and a 5-year-old to focus on routine and follow-up studies in paediatric patients. Our study used a CT scanner manufactured by a single manufacturer. The relationship between tube voltage, image noise, radiation dose, and phantom size may depend, to a certain degree, on CT scanner specifications, which may vary between manufacturers. To screen for congenital heart disease, our focus was exclusively on thoracic CT scans. Most paediatric scans are performed with a 3-mm slice thickness; we used a 5-mm slice thickness. Further studies with a slice thickness of 3 mm are required to confirm our hypothesis.

Conclusion

Compared with that observed for the 80-mm collimation, the dose deposited outside the imaged volume (to the lens and thyroid) was significantly lower in newborn and 5-year-old phantoms with 40-mm collimation during thoracic helical CT scans.

Supplementary Information The online version contains supplementary material available at https://doi.org/10.1007/s00247-024-05862-3.

Author contribution T.M. contributed to the study design, data collection, algorithm construction, image evaluation, and the writing and editing of the article; M.K., C.F., T.O., and T.I. carried out the data collection, image evaluation, and the reviewing and editing of the article; Y.K., T.Y., and S.A. performed supervision, project administration, image evaluation, and reviewing and editing of the article. All authors read and approved the final manuscript.

Funding This work was supported in part by an Academic Research Grant (2021–2022) from the Japanese Society of Radiological Technology.

Data availability All data is available in the Supplementary Material.

Declarations

Ethics approval Not applicable to this phantom study.

Conflicts of interest None

References

1. Hsiao EM, Rybicki FJ, Steigner M (2010) CT coronary angiography: 256-slice and 320-detector row scanners. Curr Cardiol Rep 12:68–75
2. Nagayama Y, Oda S, Nakaura T, Tsuji A, Urata J, Furusawa M, Utsunomiya D, Funama Y, Kidoh M, Yamashita Y (2018) Radiation dose reduction at pediatric CT: use of low tube voltage and iterative reconstruction. Radiographics: a review publication of the Radiological Society of North America. Inc 38:1421–1440
3. Nagayama Y, Sakabe D, Goto M, Emoto T, Oda S, Nakaura T, Kidoh M, Uetani H, Funama Y, Hirai T (2021) Deep learning-based reconstruction for lower-dose pediatric CT: technical principles, image characteristics, and clinical implementations. Radiographics: a review publication of the Radiological Society of North America. Inc 41:1936–1953
4. Zhu Y, Li Z, Ma J, Hong Y, Pi Z, Qu X, Xu M, Li J, Zhou H (2018) Imaging the infant chest without sedation: feasibility of using single axial rotation with 16-cm wide-detector CT. Radiology 286:279–285
5. Zhu Y, Pi Z, Zhou H, Li Z, Lei F, Hui J, Zhang X, Xie J, Liang Y (2021) Imaging pediatric acute head trauma using 100-kVp low dose CT with adaptive statistical iterative reconstruction (ASIR-V) in single rotation on a 16 cm wide-detector CT. J Xray Sci Technol 29:517–527
6. Westra SJ (2019) High-pitch CT, decreasing need for sedation and its potential side effects: some practical considerations and future directions. Pediatr Radiol 49:297–300
7. Apfaltrer G, Albrecht MH, Schoepf UJ, Duguay TM, De Cecco CN, Nance JW, De Santis D, Apfaltrer P, Eid MH, Eason CD, Thompson ZM, Bauer MJ, Varga-Szemes A, Jacobs BE, Sorantin E, Tesche C (2018) High-pitch low-voltage CT coronary artery calcium scoring with tin filtration: accuracy and radiation dose reduction. Eur Radiol 28:3097–3104
8. Maeda E, Shirota G, Shibata E, Komatsu S, Ino K, Torigoe R, Abe O (2020) Comparison of image quality between synthetic and patients' electrocardiogram-gated 320-row pediatric cardiac computed tomography. Pediatr Radiol 50:180–187
9. Shirota G, Maeda E, Namiki Y, Bari R, Ino K, Torigoe R, Abe O (2017) Pediatric 320-row cardiac computed tomography using electrocardiogram-gated model-based full iterative reconstruction. Pediatr Radiol 47:1463–1470
10. Goo HW, Siripornpitak S, Chen SJ, Lilyasari O, Zhong YM, Latiff HA, Maeda E, Kim YJ, Tsai IC, Seo DM (2021) Pediatric cardiothoracic CT guideline provided by the Asian Society of Cardiovascular Imaging Congenital Heart Disease Study Group: Part 2. Contemporary clinical applications. Korean J Radiol 22:1397–1415
11. Cohnen M, Poll LJ, Puettmann C, Ewen K, Saleh A, Mödder U (2003) Effective doses in standard protocols for multi-slice CT scanning. Eur Radiol 13:1148–1153
12. Theocharopoulos N, Damilakis J, Perisinakis K, Gourtsoyiannis N (2007) Energy imparted-based estimates of the effect of z overscanning on adult and pediatric patient effective doses from multi-slice computed tomography. Med Phys 34:1139–1152
13. Tzedakis A, Damilakis J, Perisinakis K, Stratakis J, Gourtsoyiannis N (2005) The effect of z overscanning on patient effective dose from multidetector helical computed tomography examinations. Med Phys 32:1621–1629
14. Tzedakis A, Perisinakis K, Raissaki M, Damilakis J (2006) The effect of z overscanning on radiation burden of pediatric patients undergoing head CT with multidetector scanners: a Monte Carlo study. Med Phys 33:2472–2478
15. Tzedakis A, Damilakis J, Perisinakis K, Karantanas A, Karabekios S, Gourtsoyiannis N (2007) Influence of z overscanning on normalized effective doses calculated for pediatric patients undergoing multidetector CT examinations. Med Phys 34:1163–1175
16. Fuchs TO, Kachelriess M, Kalender WA (2000) System performance of multislice spiral computed tomography. IEEE Eng Med Biol Mag 19:63–70
17. Taguchi K, Aradate H (1998) Algorithm for image reconstruction in multi-slice helical CT. Med Phys 25:550–561
18. Urikura A, Hara T, Yoshida T, Nishimaru E, Hoshino T, Nakaya Y, Endo M (2019) Overranging and overbeaming measurement in area detector computed tomography: a method for simultaneous measurement in volume helical acquisition. J Appl Clin Med Phys 20:160–165
19. Vano E, Kleiman NJ, Duran A, Rehani MM, Echeverri D, Cabrera M (2010) Radiation cataract risk in interventional cardiology personnel. Radiat Res 174:490–495
20. Ainsbury EA, Bouffler SD, Dörr W, Graw J, Muirhead CR, Edwards AA, Cooper J (2009) Radiation cataractogenesis: a review of recent studies. Radiat Res 172:1–9
21. Nakashima E, Neriishi K, Minamoto A (2006) A reanalysis of atomic-bomb cataract data, 2000–2002: a threshold analysis. Health Phys 90:154–160
22. Neriishi K, Nakashima E, Minamoto A, Fujiwara S, Akahoshi M, Mishima HK, Kitaoka T, Shore RE (2007) Postoperative cataract cases among atomic bomb survivors: radiation dose response and threshold. Radiat Res 168:404–408
23. Worgul BV, Kundiyev YI, Sergiyenko NM, Chumak VV, Vitte PM, Medvedovsky C, Bakhanova EV, Junk AK, Kyrychenko OY, Musijachenko NV, Shylo SA, Vitte OP, Xu S, Xue X, Shore RE (2007) Cataracts among Chernobyl clean-up workers: implications regarding permissible eye exposures. Radiat Res 167:233–243
24. (2007) The 2007 Recommendations of the International Commission on Radiological Protection. ICRP publication 103. Ann ICRP 37:1–332
25. Iglesias ML, Schmidt A, Ghuzlan AA, Lacroix L, Vathaire F, Chevillard S, Schlumberger M (2017) Radiation exposure and thyroid cancer: a review. Arch Endocrinol Metab 61:180–187
26. Booij R, Dijkshoorn ML, van Straten M (2017) Efficacy of a dynamic collimator for overranging dose reduction in a second- and third-generation dual source CT scanner. Eur Radiol 27:3618–3624
27. Deak PD, Langner O, Lell M, Kalender WA (2009) Effects of adaptive section collimation on patient radiation dose in multisection spiral CT. Radiology 252:140–147
28. Schilham A, van der Molen AJ, Prokop M, de Jong HW (2010) Overranging at multisection CT: an underestimated source of excess radiation exposure. Radiographics : a review publication of the Radiological Society of North America, Inc 30:1057–1067
29. Lee T, Tsai IC, Fu YC, Jan SL, Wang CC, Chang Y, Chen MC (2006) Using multidetector-row CT in neonates with complex congenital heart disease to replace diagnostic cardiac catheterization for anatomical investigation: initial experiences in technical and clinical feasibility. Pediatr Radiol 36:1273–1282